



**HAL**  
open science

## ricin b lectin-like proteins of the microsporidian encephalitozoon cuniculi and anncaliia algerae are involved in host-cell invasion

Nastasia Prybylski, Maurine Fayet, Aurore Dubuffet, Frédéric Delbac, Ayhan Kocer, Christine Gardarin, Philippe Michaud, Hicham El Alaoui, Pascal Dubessay

### ► To cite this version:

Nastasia Prybylski, Maurine Fayet, Aurore Dubuffet, Frédéric Delbac, Ayhan Kocer, et al.. ricin b lectin-like proteins of the microsporidian encephalitozoon cuniculi and anncaliia algerae are involved in host-cell invasion. Parasitology International, 2022, 87, pp.102518. 10.1016/j.parint.2021.102518 . hal-03925737

**HAL Id: hal-03925737**

**<https://hal.science/hal-03925737v1>**

Submitted on 8 Jan 2024

**HAL** is a multi-disciplinary open access archive for the deposit and dissemination of scientific research documents, whether they are published or not. The documents may come from teaching and research institutions in France or abroad, or from public or private research centers.

L'archive ouverte pluridisciplinaire **HAL**, est destinée au dépôt et à la diffusion de documents scientifiques de niveau recherche, publiés ou non, émanant des établissements d'enseignement et de recherche français ou étrangers, des laboratoires publics ou privés.



Distributed under a Creative Commons Attribution - NonCommercial 4.0 International License



26 *cuniculi* genomes were screened by bioinformatic analysis to identify proteins with an  
27 extracellular prediction and possessing RBL-type carbohydrate-binding domains,  
28 being both potentially relevant factors contributing to host cell adherence. Three  
29 proteins named AaRBL-1 and AaRBL-2 from *A. algerae* and EcRBL-1 from *E.*  
30 *cuniculi*, were selected and comparative analysis of sequences suggested their  
31 belonging to a multigenic family, with a conserved structural RBL domain despite a  
32 significant amino acid sequence divergence. The production of recombinant proteins  
33 and antibodies against the three proteins allowed their subcellular localization on the  
34 spore wall and/or the polar tube. Adherence inhibition assays based on pre-  
35 treatments with recombinant proteins or antibodies highlighted the significant  
36 decrease of the proliferation of both *E. cuniculi* and *A. algerae*, strongly suggesting  
37 that these proteins are involved in the infection process.

38

39 Key words: Microsporidia, *Encephalitozoon cuniculi*, *Anncaliia algerae*, invasion,  
40 Ricin-B lectin, adherence

41

## 42 **1. Introduction**

43 Microsporidia are obligate intracellular eukaryotic parasites including over 200  
44 genera and 1400 species that have been characterized [1]. Microsporidia were  
45 identified more than 150 years ago as etiologic agent of the Pebrine disease in  
46 silkworms with the identification of *Nosema bombycis* [2]. Microsporidia can infect a  
47 wide variety of hosts ranging from invertebrates to vertebrates and are reported to be  
48 involved in protists and in all major groups of animals, including human [3,4]. Thus,  
49 Microsporidia can cause significant economic losses in fish and shrimp farming,  
50 sericulture and beekeeping [5–7]. Microsporidia are phylogenetically classified to

51 Fungi, either as a basal branch of the Fungi or as a sister group [8–10], and most  
52 likely related to the Cryptomycota [11,12].

53 The life cycle of Microsporidia is divided into three phases including the  
54 infective phase, the proliferative phase and the sporogonial phase. The spore  
55 constitutes the infective stage, and the only extracellular form of the parasite, able to  
56 persist in the environment for months thanks to a resistant thick two-layered wall and  
57 contributing to the parasite dissemination [4,13,14]. Microsporidia infect host cells  
58 through a unique and highly specialized invasion process, involving a tubular  
59 structure coiled within the spore termed the polar tube. After spore discharge, the  
60 extruded polar tube is used for inoculating the infective sporoplasm into the host cell  
61 cytoplasm, in which the parasite proliferation takes place [15–17]. Spore discharge  
62 occurs in different steps, including (i) an activation phase, (ii) the increase of the  
63 intrasporal osmotic pressure, (iii) the eversion of the polar tube and (iv) the passage  
64 of the sporoplasm through the polar tube. However, the exact mechanism(s) of this  
65 process is not well understood [18]. The conditions triggering spore activation widely  
66 differ according to species. Some factors promoting spore discharge are determined  
67 such as shift in environmental pH [19,20] or the concentration of various cations or  
68 anions [20,21].

69 At least three major routes seem to be involved in host cell invasion by  
70 Microsporidia, (i) adherence of spores to host cell receptors prior to polar tube  
71 evagination, (ii) extrusion of polar tube piercing the host cell plasma membrane or (iii)  
72 phagocytosis of the spore followed by the extrusion of the polar tube [22]. Several  
73 studies have demonstrated the importance of some proteins in the infection process,  
74 in particular in the adherence and spore germination processes. Both Spore Wall  
75 Proteins (SWP) and Polar Tube Proteins (PTP) play a major role during the first



76 interactions between Microsporidia and host cell components. A few SWPs  
77 interacting with heparin-like motifs and glycosaminoglycans were identified from  
78 several microsporidian species such as *Encephalitozoon* spp., *N. bombycis* and  
79 *Antonospora locustae* [23–28]. The spore wall EnP1 protein containing a heparin-  
80 binding domain in both *Encephalitozoon cuniculi* and *Encephalitozoon intestinalis*,  
81 was identified as a major functional element of the adherence process to host cells.  
82 The use of exogenous recombinant proteins EnP1 or rabbit anti-EnP1 antibodies  
83 decreased the adherence of the spore to host cells and subsequent infection [27]. In  
84 addition, a variety of exogenous sulfated glycans have been shown to inhibit  
85 *Encephalitozoon* spore invasion into host cells, probably by blocking adherence  
86 process [25,27]. A gene encoding a protein associated to the ADAM (disintegrin and  
87 metalloprotease) family of type I transmembrane glycoprotein was also identified in  
88 the *E. cuniculi* genome. ADAM proteins are known to be involved in a variety of  
89 biological processes such as cell adherence and proteolysis. The use of exogenous  
90 recombinant MsADAM protein (Microsporidia ADAM) inhibited the adherence of *E.*  
91 *intestinalis* spores to host cells but also reduced host cell infection by ~20%,  
92 suggesting its role in both adherence and infection processes [29].

93         Some studies were conducted to characterize receptors localized on host cell  
94 surface. The NbSWP26 in *N. bombycis* was demonstrated to interact with the  
95 immunoglobulin-like protein BmTLP of silkworm *Bombyx mori*, highlighting its crucial  
96 role in spore invasion of silkworm cells [30]. The *Encephalitozoon hellem* Polar Tube  
97 Protein PTP4 was shown to be able to bind *in vitro* to the host cell surface via the  
98 host transferrin receptor 1 (TfR1) protein. Interestingly, interfering with the  
99 interactions between PTP4 and TfR1 led to a decrease in the infection of host cells  
100 [31]. In a few microsporidian species such as *Spraguea lophii* and *N. bombycis*,

101 proteins containing a Ricin-B Lectin (RBL) domain were identified and their  
102 involvement in parasite infection has been suggested or demonstrated [32,33]. Ricin  
103 is a lectin glycoprotein composed of a chain A and a chain B linked by a disulfide  
104 bond [34]. The B chain is a lectin that binds to cells through interactions with  
105 glycolipids and glycoproteins in particular with  $\beta$ -linked galactose or *N*-  
106 acetylgalactosamine containing glycans localized at the cell surface [35,36]. The  
107 functionality of the *NbRBL* on the adherence and infection was demonstrated by  
108 incubating anti-*NbRBL* antibodies with host cells and *N. bombycis* spores. The  
109 results showed a significant reduction of the spore infectivity associated to a  
110 decreased adherence of spores to host cells [33].

111 Lectins are biologically active proteins isolated from humans, animals, plants and  
112 microorganisms. Their ability to specifically bind different types of carbohydrates and  
113 their widespread occurrence suggests their importance in various cellular processes  
114 such as cell adherence, apoptosis and proliferation [37]. For example, the bacteria  
115 *Bordetella pertussis*, responsible of a highly contagious respiratory infectious  
116 disease, possesses a filamentous hemagglutinin that promotes strong attachment of  
117 the bacteria to host cells [38–40]. The attachment of *Plasmodium falciparum*  
118 merozoites to erythrocytes, leading to invasion, is mediated by a parasite adhesin  
119 called EBA-175 [41,42]. Regarding viruses, the influenza virus also possesses  
120 hemagglutinin involved in binding to sialic acids at the host cell surface. Endocytosis  
121 is a prerequisite before the fusion of the viral envelope with host endosomal  
122 membrane followed by the uptake of the virus into the cell [42–44]. All these data  
123 argue for an important role of pathogen adherence prior to host cell invasion.

124 In this study, by using bioinformatic tools and preliminary experimental data,  
125 we selected some proteins predicted to be extracellular and possessing

126 carbohydrate-binding domains that constitute good candidates for host cell  
127 adherence in *E. cuniculi*, parasite of mammals including humans and *Anncaliia*  
128 *algerae*, parasite of humans and mosquitoes. Thus, two Ricin B Lectin-Like (RBLL)  
129 proteins from *A. algerae*, AaRBLL-1 and AaRBLL-2 and one from *E. cuniculi*,  
130 EcRBLL-1 were selected, partly on the basis of the occurrence of a Ricin-B Lectin  
131 domain in their amino acid sequences. Recombinant proteins were produced in  
132 bacteria or yeast in order to obtain specific antibodies that were used to localize  
133 these proteins on the microsporidian spore. Recombinant proteins and mouse  
134 polyclonal antibodies were then used to evaluate the involvement of microsporidian  
135 RBLL proteins in adherence and infection using adherence inhibition assays.

136

## 137 **2. Materials and methods**

### 138 **2.1 Cells, reagents and parasite culture**

139 Human Fetal Fibroblasts (MRC-5) cells (ATCC CCL-171) and Human Foreskin  
140 Fibroblasts (HFF) cells (ATCC SCRC-1041) were cultured in Minimum Essential  
141 Medium Eagle (MEM) (Invitrogen) supplemented with 10% inactivated Fetal Bovine  
142 Serum (FBS) (Invitrogen), 2 mM glutamine (Gibco), 2.5  $\mu\text{g mL}^{-1}$  amphotericin B  
143 (Dutscher), 100  $\mu\text{g mL}^{-1}$  kanamycin (Pan Biotech), 25  $\mu\text{g mL}^{-1}$  gentamicin (Gibco) at  
144 37°C in a humidified 5% CO<sub>2</sub> atmosphere.

145 *E. cuniculi* and *A. algerae* cultures were maintained in Madin-Darby Canine Kidney  
146 (MDCK) cells (ATCC CCL-34) and Rabbit kidney (RK13) cells (ATCC CCL-37)  
147 respectively. Confluent monolayers of cells were infected with  $5 \times 10^5$  spores of either  
148 *E. cuniculi* or *A. algerae* in T75 flasks. The spores were collected from culture media,  
149 purified by passing through 3  $\mu\text{m}$  size filters (Millipore) for *E. cuniculi* and washed  
150 with sterile water for *A. algerae* to remove host cells. Spores were then concentrated

151 at 1600 x g, and stored in phosphate buffered saline (PBS) at 4°C. Spores used in  
152 these experiments were counted using a Kova-cell chamber. MDCK and RK13 cells  
153 were used for parasite production as they correspond to long-term production  
154 systems. However, for the following growth inhibition assays, we used MRC5 and  
155 HFF cells for *E. cuniculi* and *A. algerae* respectively, as they enabled a significant  
156 parasite production in few days.

157

## 158 **2.2 Bioinformatics analysis**

159 *E. cuniculi* and *A. algerae* local and online protein databases  
160 (<https://microsporidiadb.org/micro/>) (version June 2020) were screened using cellular  
161 localization prediction tools. The selection of proteins with a potential localization at  
162 cell surface was based on the presence of a predicted signal peptide (SignalP  
163 algorithm (<http://www.cbs.dtu.dk/services/SignalP/>)) and/or subcellular localization  
164 (WoLF PSORT algorithm (<https://wolfsort.hgc.jp>) (version June 2020). Protein motif  
165 prediction (carbohydrate binding domain) was carried out using ExPaSy proteomic  
166 tools such as InterPro (<http://www.expasy.org/tools/>). Prediction of the structure and  
167 function of the selected proteins was done using the free software Phyre2 tool  
168 (<http://www.sbg.bio.ic.ac.uk/~phyre2/html/page.cgi?id=index>). 3D model were  
169 obtained using Ezmol tool (<http://www.sbg.bio.ic.ac.uk/ezmol/>).

170 However, AaRBLL-1 was not selected by informatics tools as no peptide signal was  
171 detected and no extracellular location was predicted. Indeed, this protein was  
172 obtained from a shaving approach consisting of surface protein recovering using soft  
173 SDS lysis of spore combining with mass spectrometry analysis (Prybylski *et al.*, *in*  
174 preparation).

175

## 176 **2.3 Recombinant RBLL protein production and purification**

177 The recombinant proteins were produced in *Pichia pastoris* (strain KM71H,  
178 Invitrogen) for EcRBLL-1 and in *Escherichia coli* BL21-λDE3 (PROMEGA) for  
179 AaRBLL-1 and AaRBLL-2.

180 The EcRBLL-1 gene (Gene Bank Accession N°: ECU08\_1730) was PCR-amplified  
181 from *E. cuniculi* genomic DNA using the forward primer 5'-  
182 gggaattcGAAAATTCCTCATTAACAATAAC-3' and the reverse primer 5'-  
183 ggctcgagccgTTAAACAATGAGACAGTCACTA-3', containing respectively *Eco*RI and  
184 *Sac*II restriction sites (underlined). After digestion, the purified PCR product was  
185 inserted into the corresponding sites of pPICZα-A vector (Invitrogen) and transformed  
186 into *E. coli* (DH5-α). Plasmids from positive clones were purified and sequenced. After  
187 linearization with the *Sac*I enzyme, plasmids were used to transform *P. pastoris*  
188 *KMH71* using EasySelect *Pichia* kit (Invitrogen), and recombinant yeasts were  
189 selected on YPDS- agar plates containing zeocin antibiotic (250 μg.mL<sup>-1</sup>). The culture  
190 and production steps were carried out according to manufacturer recommendations  
191 (Invitrogen). Briefly, recombinant yeasts were cultivated at 30°C in BMGY medium  
192 (1% yeast extract; 2% peptone; 100 mM of potassium phosphate, pH 6.0; 1.34%  
193 YNB (Yeast Nitrogen Base); 4x10<sup>-5</sup>% biotin; 1% glycerol) during 16h until reaching ~4  
194 OD<sub>600</sub>. BMGY medium was then removed by centrifugation, and yeast cells were re-  
195 suspended in the induction medium, BMMY (identical to BMGY except that glycerol  
196 was replaced with methanol 0.5%). The induction of the recombinant protein  
197 expression was carried out for 72h with methanol addition every 24h. The  
198 supernatant of the culture was collected by centrifugation at 4000 xg for 10 min, and  
199 the volume was reduced to 20 mL on 3 kDa ultrafiltration membrane using Stirred  
200 Ultrafiltration Cell (Millipore®), to concentrate the recombinant proteins. Proteins

201 were then purified by Ion Metal Chromatography Affinity (IMAC) (Protino® Ni-NTA,  
202 Macherey-Nagel®), and analyzed by SDS-PAGE (12%, wt/vol.).

203 In support of GenBank sequence database related to *AaRBLL-1* (GenBank  
204 Accession N°: MZ547653) and *AaRBLL-2* (GenBank Accession N°: MZ547654), the  
205 genes were obtained by PCR amplification from *A. algerae* genomic DNA, using the  
206 primers 5'-gggatccTTTGTAATACAGGAAAGAAGCAC-3' and 5'-  
207 gggctcgagCTATTTCCGAGCAAAGAGGC-3' for *AaRBLL-1* and 5'-  
208 gggggatccATGCTGATATTTTTCTTAAGTATC-3' and 5'-  
209 gggctcgagTTACATTCCCATTGATTTAAAACAT-3' for *AaRBLL-2*. The *Bam*HI and  
210 *Xho*I restriction sites (underlined) were added at the 5' end of both primers, allowing  
211 the insertion of PCR products into the pET28a plasmid (Novagen) to generate  
212 pET28a-*AaRBLL-1* and pET28a-*AaRBLL-2*. After transformation of *E. coli* DH5α  
213 strain and selection on LB-agar (kanamycin 30 µg.mL<sup>-1</sup>) plates, plasmid DNA of  
214 positive clones were purified and sequenced, and then transformed into *E. coli* BL21-  
215 λDE3 strain for the expression of recombinant proteins. The expression was induced  
216 with IsopropylThioGalactoside (IPTG) 1mM for 4h from a culture in exponential  
217 growth (OD<sub>600</sub> ~ 0.4 - 0.6). Recombinant proteins were then purified by Ion Metal  
218 Chromatography Affinity (IMAC) (Protino® Ni-NTA, Macherey-Nagel®), and analyzed  
219 by SDS-PAGE (12%, wt/vol.).

220

## 221 **2.4 Polyclonal antibody production and immunoblotting**

222 Polyclonal antibodies against each recombinant *EcRBLL-1* (*recEcRBLL-1*); *AaRBLL-*  
223 *1* (*recAaRBLL-1*) and *AaRBLL-2* (*recAaRBLL-2*) protein were obtained after  
224 immunization of BALB/c mice. Mice were initially immunized with 100 µg of each  
225 purified protein emulsified with Freund's complete adjuvant (Sigma) in the peritoneum

226 followed by four other injections of each purified protein emulsified with Freund's  
227 incomplete adjuvant (Sigma). The serum was collected one week after the last  
228 injection and stored at -20°C. For immunoblotting, *E. cuniculi* and *A. algerae* proteins  
229 were extracted as follows: spores in Laemmli buffer (10% Glycerol, 2% SDS, 62.5  
230 mM Tris-Base pH 6.8, 0.0025% bromophenol blue, 100 mM DTT) were subjected to  
231 10 cycles of freezing-thawing cycles followed by 15 min of boiling. The sample was  
232 centrifuged 2 min at 14 000 *xg*. Total protein extract was collected by centrifugation  
233 at 14 000 *xg* for 5 min. Proteins were then separated by SDS-PAGE 12%, transferred  
234 onto polyvinylidene difluoride (PVDF) membranes (Merck), and blocked with a  
235 solution of PBS-milk 5% overnight at 4°C. Membranes were incubated with either  
236 anti-*Ec*RBLL-1, anti-*Aa*RBLL-1 and anti-*Aa*RBLL-2 (1:200 dilution) for 2 hours at  
237 37°C. The secondary antibody, a goat anti-mouse IgG (H+L), HRP Conjugate  
238 (Promega) was incubated for 1 hour at RT. Membranes were revealed by  
239 chemiluminescence using the Clarity Western ECL Substrate kit (Biorad).

240

## 241 **2.5 Immunolocalization assays (IFA) on purified spores of *E. cuniculi* and *A.*** 242 ***algerae***

243 Purified spores were fixed in PFA 4% for 20 minutes at 4°C. Purified spores were  
244 incubated with glycine 0.1M for 5 min at RT. After a quick wash with PBS, a  
245 saturation step was performed with a blocking solution (PBS-bovine albumin serum  
246 (BSA) 1%, (wt/vol)) for one hour at RT.

247 For purified *E. cuniculi* spores, a first immunolabeling was done by incubating the  
248 samples with a 1:100 dilution of anti-*Ec*RBLL-1 mouse polyclonal antibodies for two  
249 hours at RT, then washed with 0.1% Triton X100-PBS and incubated for an  
250 additional hour at RT with a 1:1000 dilution of mouse IgG (H+L) secondary antibody,

251 Alexa Fluor 555 conjugate (Invitrogen). In a second time, the samples were  
252 incubated with a 1:500 dilution of anti-*E. cuniculi* rabbit serum (from a naturally  
253 infected rabbit) for one hour at RT, then washed with 0.1% Triton X100-PBS and  
254 incubated for an additional hour at RT with a 1:1000 dilution of rabbit IgG (H+L)  
255 secondary antibody, Alexa Fluor 488 conjugate (Invitrogen).

256 For purified *A. algerae* spores, samples were incubated with antibodies against  
257 AaRBLL-1 or AaRBLL-2 at 1:100 for 2 hours at RT. Samples were then washed with  
258 PBS and incubated for an hour at RT with a 1:1000 dilution of mouse IgG (H+L)  
259 secondary antibody, Alexa Fluor 555 conjugate.

260 A staining of the genetic material of spores was performed with DAPI (4',6-diamidino-  
261 2-phenylindole) at 100  $\mu\text{g}\cdot\text{mL}^{-1}$  for 5 min at RT. Coverslips were mounted with  
262 Prolong Diamond Antifade Mounting (Invitrogen) and preparations were then  
263 observed with an epifluorescence microscope, magnification factor x 100 (LEICA DM  
264 IRB).

265

## 266 **2.6 Cytotoxic assay**

267 Human Fibroblast (MRC-5 or HFF) cells were seeded in 96-well-microplates at a  
268 density of  $2 \times 10^4$  cells/well in MEM medium supplemented with 10% inactivated  
269 FBS, 2 mM glutamine, 2.5  $\mu\text{g}\cdot\text{mL}^{-1}$  amphotericin B, 100  $\mu\text{g}\cdot\text{mL}^{-1}$  kanamycin, 25  $\mu\text{g}\cdot\text{mL}^{-1}$   
270 gentamicin at 37°C in a humidified 5% CO<sub>2</sub> atmosphere for approximately 48 h  
271 to reach confluence. The medium was then replaced by fresh culture medium  
272 containing different concentrations of the recombinant proteins recEcRBLL-1 and  
273 recAaRBLL-2 (25  $\mu\text{g}\cdot\text{mL}^{-1}$ ), or anti-EcRBLL-1, anti-AaRBLL-1 and anti-AaRBLL-2  
274 mouse polyclonal antibodies (1:100) to evaluate their cytotoxicity on human cells.  
275 Negative control (cells with culture medium only) and positive control (cells with 20%



276 DMSO diluted in medium) were also added to each 96-well culture plate. Each  
277 condition was tested in triplicate. After incubation for 7 days at 37°C in a humidified  
278 5% CO<sub>2</sub> atmosphere, the medium was removed and replaced by tetrazolium dye  
279 MTT (3-(4,5-dimethylthiazol-2-yl)-2,5-diphenyltetrazolium bromide) (Sigma Aldrich) at  
280 a 1:10 dilution in culture medium. Microplates were then incubated at 37°C for 2 h  
281 under slight shaking. The dye and medium were replaced by a solution of  
282 DMSO:Isopropanol (1/1, v/v) and incubated for 5 min at room temperature to dissolve  
283 the protein-bound dye for OD at 550 nm using a microplate reader (Multiskan FC,  
284 ThermoScientific). The cytotoxic effect of the recombinant proteins and polyclonal  
285 antibodies on host cells was analyzed by comparing to the negative control  
286 corresponding to 100% cell growth using a Wilcoxon test a non-parametric test with R  
287 studio software. Differences were considered significant if the *p* value was <0.05.

288

## 289 **2.7 *In vitro* growth inhibition assays**

290 The potential involvement of *EcRBLL-1*, *AaRBLL-1* and *AaRBLL-2* proteins in the  
291 infection process was addressed through inhibition tests, aiming to block the  
292 interaction between these proteins and their interactants at host cell surface, using  
293 antibodies as blocking agents or recombinant proteins as competitors.

294

### 295 **2.7.1 Effects of Anti-*EcRBLL-1* and rec*EcRBLL-1***

296 After validation of non-cytotoxic effect of rec*EcRBLL-1* and anti-*EcRBLL-1* antibodies,  
297 the anti-microsporidian assay was performed using non-cytotoxic concentrations of  
298 the rec*EcRBLL-1* (25 µg mL<sup>-1</sup>) and anti-*EcRBLL-1* antibodies (1:100) on *E. cuniculi*-  
299 infected MRC-5 cells. Host cells were first seeded in 48 well culture plates at a  
300 density of 4 x 10<sup>4</sup> cells/well in the same culture medium described above. Cells were

301 allowed to grow at 37°C in a humidified 5% CO<sub>2</sub> atmosphere. Triplicates wells per  
302 condition were created on the plate: (i) uninfected control group, (ii) infected control  
303 group, (iii) infected group exposed to the diluted rec*Ec*RBLL-1 and (iv) infected group  
304 exposed to the diluted anti-*Ec*RBLL-1. The uninfected control group in each plate  
305 allowed measuring the background signal in the ELISA assay. When cells reached  
306 confluence, the medium was replaced by fresh culture medium containing or not  
307 rec*Ec*RBLL-1 for one hour at 37°C. Meanwhile, *E. cuniculi* spores were pretreated  
308 with anti-*Ec*RBLL-1 antibodies and incubated at 37°C for 1 h. After the incubation  
309 time, 2 x 10<sup>5</sup> spores of *E. cuniculi* were added to the pretreated cells with  
310 rec*Ec*RBLL-1 for an hour. Pretreated spores were also put in contact with host cells  
311 for one hour. Culture medium was removed, cells were gently rinsed with PBS and  
312 fresh culture medium was added to each well. After 7 days, the culture medium was  
313 removed and cells were fixed with methanol at -20°C for 30 min. Methanol was  
314 removed and after a quick wash of the cells with PBS, cells were saturated with 100  
315 mM Tris-2% BSA (Sigma-Aldrich) overnight. Then cells were incubated at 37°C for 1  
316 h with an anti-*E. cuniculi* rabbit serum (from naturally infected rabbit) diluted at  
317 1:1000 in a dilution buffer (10 mM Tris pH = 8, 150 mM NaCl, 0.05% Tween 20, 0.2%  
318 BSA Sigma-Aldrich). Cells were washed five times with washing buffer (10 mM Tris  
319 pH = 8, 0.05% Tween 20) and incubated at 37°C for 1h with an anti-rabbit antibody  
320 (Anti-Rabbit IgG AP Conjugate, Promega) diluted at 1:10 000 in antibody dilution  
321 buffer. The cells were washed five times with washing buffer and the substrate  
322 solution (0.1 mM 4-méthylumbelliferyl phosphate (MUP), 1 mM MgCl<sub>2</sub>, 50 mM  
323 Na<sub>2</sub>CO<sub>3</sub> pH = 9.8; Sigma-Aldrich) was added. After incubation at 37°C for 30 min  
324 under slight shaking, the reaction was stopped by the addition of 3 M NaOH and the

325 fluorescence was measured with a Fluoroskan Ascent FL, using excitation and  
326 detection wavelengths of 355 nm and 460 nm, respectively.

327

### 328 **2.7.2 Effects of Anti-AaRBLL-1, anti-AaRBLL-2 and recAaRBLL-2**

329 HFF cells were seeded on coverslips at a density of  $10^5$  cells per well in 24 well  
330 culture plates in the same culture medium described above.

331 Once confluence was reached, on one side cells were pretreated with recAaRBLL-2  
332 ( $25 \mu\text{g mL}^{-1}$ ) for one hour at  $30^\circ\text{C}$  in culture medium. After the incubation time, cells  
333 were put in contact with  $3 \times 10^5$  spores of *A. algerae* for one hour. Culture medium  
334 was then removed, cells were gently rinsed with PBS and fresh culture medium was  
335 added to each well.

336 On the other side,  $3 \times 10^5$  spores were pretreated with either anti-AaRBLL-1 or anti-  
337 AaRBLL-2 antibodies (1:100) for an hour at  $30^\circ\text{C}$ . Pretreated spores were then put in  
338 contact with host cells for an hour. Culture medium was removed, cells were gently  
339 rinsed with PBS and fresh culture medium was added to each well. Triplicate wells  
340 were done on each plate.

341 After 7 days of incubation at  $30^\circ\text{C}$  in a humidified 5%  $\text{CO}_2$  atmosphere, the culture  
342 medium was removed and cells were fixed in PFA 4% at  $4^\circ\text{C}$  for 20 min. The  
343 observation and quantification of infectious foci was done using fluorescence *in situ*  
344 hybridization (FISH) method.

345 A post fixation was done in 50% ethanol for 15 min followed by ethanol 100M for 10  
346 min. After two wash of 15 min in PBS, a pre-hybridization was done in a solution  
347 PBS: hybridization buffer (TH) (20 mM Tris-HCl pH 7.8; 0.9 M NaCl; 1X Denhardt's  
348 solution (VWR Life Science) and 0.01% SDS for 15 min at room temperature,  
349 followed by a 15 min incubation in TH solution. A last incubation in TH solution was

350 done for 20 min at 45°C. TH solution was replaced by the hybridization solution  
351 containing 5'-Cy3-labeled *ssuRNA A. algerae* specific-probe (Eurofins)  
352 GTACTATCCAGTCCGCTC-3' (ANN01-Cy3) (50 µM ANN01-Cy3 probe and 0.5 µM  
353 of warmed TH at 45°C). Plates were placed at 45°C for 3 h. After this incubation, the  
354 hybridization solution was removed and **two** 30 min-washes with warmed TH solution  
355 were done. TH solution was replaced with PBS. DNA was stained with DAPI for 30  
356 min. Coverslips were mounted with Prolong Diamond Antifade Mounting. The  
357 percentage of infected cells was assessed by counting cell nuclei and infectious foci  
358 in 10 randomly chosen fields from each coverslip.

359

### 360 **2.7.3 Statistical analysis**

361 The effects of *recEcRBLL-1* and *recAaRBLL-2* or anti-*EcRBLL-1*; anti-*AaRBLL-1* and  
362 anti-*AaRBLL-2* polyclonal antibodies on the infection of host cells by either *E. cuniculi*  
363 or *A. algerae* were analyzed by comparing to the infected control corresponding to  
364 100% parasite growth of each independent experiment using a Wilcox test, a non-  
365 parametric test with R studio software. For each independent experiment, infected  
366 control was compared to each condition in order to determine if a significant  
367 difference was observed. Differences were considered significant if the *p* value was  
368 <0.05 and highly significant if the *p* value was <0.001.

369

## 370 **3. Results**

### 371 **3.1 Bioinformatic characterization of *EcRBLL-1*, *AaRBLL-1* and *AaRBLL-2***

372 Our strategy **allowed** us to identify in *E. cuniculi* a hypothetical protein, composed of  
373 214 amino acids with a predicted molecular weight (MW) of 23.4 kDa. The *EcRBLL-1*  
374 protein displayed a significant score of extracellular prediction, associated with the

375 identification of a cleavage site between the amino acids A19 and K20 related to a  
376 probable peptide signal (Fig.1A). A putative carbohydrate binding domain related to  
377 RBLL (Ricin-B lectin like) was identified in the region extending from the amino acids  
378 aa54 to aa133 (Fig. 1A). The glycosylation pattern of *EcRBLL-1* has been analyzed  
379 and has revealed the prediction of one and six potential sites for *N*-glycosylation and  
380 *O*-glycosylation respectively (Fig. 1A).

381 In the same way, two hypothetical proteins, named *AaRBLL-1*(Accession Number  
382 MZ547653) and *AaRBLL-2* (Accession Number MZ547654), were identified in *A.*  
383 *algerae*. *AaRBLL-1* and *AaRBLL-2* are composed of 202 and 181 amino acids  
384 respectively, with a deduced molecular weight of 23.4 kDa for *AaRBLL-1* and 20.2  
385 kDa for *AaRBLL-2*. No signal peptide was predicted for *AaRBLL-1* whereas *AaRBLL-*  
386 *2* displayed a peptide signal using the Microsporidia DB SignalP tool (version June  
387 2020). WoLF PSORT online software predicted a nuclear and extracellular  
388 localization for *AaRBLL-1* and *AaRBLL-2* respectively. Despite the results obtained  
389 for *AaRBLL-1*, this protein was selected according to a shaving approach, aiming  
390 at identifying *A. algerae* surface proteins (Prybylski et al., in preparation). The search  
391 of carbohydrate binding domain highlighted a RBLL domain for both *AaRBLL-1* and  
392 *AaRBLL-2* protein, localized between aa38 and aa102 and between aa65 and aa120,  
393 respectively (Fig. 1A). As for *A. algerae*, putative glycosylation sites have been  
394 predicted including only three *O*-glycosylation sites for *AaRBLL-1*, and one *N*-  
395 glycosylation and one *O*-glycosylation site for *AaRBLL-2*.

396 The similarity between the three RBLL proteins was analyzed by sequence alignment  
397 which revealed no significant homology between the protein sequences, suggesting  
398 their membership to functionally distinct proteins. Hence, the identification of a RBLL  
399 would not involve large amino acids sequence conservation, but might be associated

400 to specific secondary and tertiary structure organization. This hypothesis was  
401 confirmed by modeling 3D structure using Phyre2 software. The three RBLL were  
402 associated to similar 3D models of agglutinin and  $\beta$ -glucanase, and were shown to  
403 comprise in majority of  $\beta$ -strands and a weak percentage of  $\alpha$ -helix that are  
404 frequently found in lectins (Table 1).

405

### 406 **3.2 Polar tube and spore wall localization of *EcRBLL-1*, *AaRBLL-1* and *AaRBLL-*** 407 **2**

408 For immunolocalization experiments, polyclonal antibodies against *EcRBLL-1*,  
409 *AaRBLL-1* and *AaRBLL-2* proteins were generated by immunization of mice with  
410 recombinant proteins. The recombinant proteins were systematically performed both  
411 in *E. coli* and *P. pastoris* systems, but only the expression system allowing high level  
412 of expression and purification was retained. After purification by IMAC, the purified  
413 proteins were analyzed in SDS-PAGE, and only single band was revealed with  
414 expected sizes of about 20 kDa for recAaRBLL-2 and closed to 23 kDa for both  
415 rec*EcRBLL-1* and recAaRBLL-1. However, as recAaRBLL-1 was insoluble and  
416 purified under denaturing conditions, the recombinant protein was only used for  
417 antibody production and not as competitor for growth inhibition tests.

418 Polyclonal antibodies specificity was analyzed by Western blot ~~both~~ on spore proteins  
419 extracts ~~of both species and total proteins extracted from host cells, used as negative~~  
420 ~~controls~~. As shown in figure 1B, only a single protein band was detected at about 28  
421 kDa with anti-*EcRBLL-1* antibodies in *E. cuniculi* sporal proteins, and close to 25 kDa  
422 and 20 kDa with respectively anti-*AaRBLL-1* and anti-*AaRBLL-2* antibodies for spore  
423 proteins from *A. algerae*. ~~However, two extra bands were detected at about 35 kDa~~  
424 ~~and 30 kDa with anti-*AaRBLL-1* antibodies that could potentially correspond to other~~

425 ~~RBL proteins. Indeed, bio-informatics analysis reveals the presence of several RBL~~  
426 ~~proteins in *A. algerae* proteome close to these approximate weights (data not~~  
427 ~~shown)~~. Moreover, the fact that the reactive bands sizes **did** not match the predicted  
428 molecular weights 23 kDa for *EcRBLL-1* and *AaRBLL-2* may be attributed to their  
429 post-translational modifications such as glycosylation that was predicted on these  
430 proteins. No cross hybridization with each antibody was also observed between  
431 spore proteins from *E. cuniculi* and *A. algerae*.

432 To investigate the localization of *EcRBLL-1* in *E. cuniculi* spores, anti-*EcRBLL-1*  
433 antibodies were used for immunofluorescence analysis (IFA). A first immunolabeling  
434 was performed with the anti-*EcRBLL-1* mouse polyclonal antibodies followed by a  
435 second immunolabeling using an anti-*E. cuniculi* rabbit serum (from naturally infected  
436 rabbits). Fluorescence labeling demonstrated that anti-*EcRBLL-1* polyclonal  
437 antibodies reacted with the extruded polar tube of the spore (**Fig. 2**). As expected the  
438 anti-*Ec* rabbit serum, labeled the whole extruded polar tube as well as the spore wall  
439 of mature spores. Interestingly, the merge of anti-*Ec* rabbit serum and anti-*EcRBLL-1*  
440 fluorescences highlighted a define region ~~at the tip of the polar tube~~ only labeled with  
441 the anti-*EcRBLL-1* polyclonal antibodies. Furthermore, the quantification of the anti-  
442 *EcRBLL-1* signal intensity, confirmed the heterogeneous intensity of labeling  
443 throughout the polar tube, with a higher intensity localized at the tip of the **labeling**  
444 (**Fig. 2**). Localizations of both *AaRBLL-1* and *AaRBLL-2* in *A. algerae* spores were  
445 also analyzed by IFA using anti-*AaRBLL-1* and anti-*AaRBLL-2* polyclonal antibodies.  
446 Both *AaRBLL-1* and *AaRBLL-2* were detected on the spore wall and the polar tube.  
447 However, the labelling of the spore wall was more distinct with anti-*AaRBLL-2* than  
448 with anti-*AaRBLL-1* (**Fig. 3 and 4**).

449

450 **3.3 Decrease of adherence and infection using recombinant proteins**  
451 **recEcRBLL-1 and recAaRBLL-2, and anti-EcRBLL-1, anti-AaRBLL-1, anti-**  
452 **AaRBLL-2 antibodies as competitors of spore adherence**

453 Cytotoxic assays were performed in order to determine the cytotoxicity on host cells  
454 of the recombinant proteins recEcRBLL-1 and recAaRBLL-2 used at 25 µg.mL<sup>-1</sup> and  
455 of the anti-EcRBLL-1, anti-AaRBLL-1 and anti-AaRBLL-2 antibodies used at a  
456 dilution of 1:100. The recombinant proteins and the antibodies showed non-cytotoxic  
457 effect on MRC-5 and HFF cells corresponding to the host cells of *E. cuniculi* and *A.*  
458 *algerae* respectively (Fig. S1).

459 To further analyze the role of EcRBLL-1 in cell adherence/invasion, antibody and  
460 recombinant protein blocking assays were performed. The effect on *E. cuniculi*  
461 infection using anti-EcRBLL-1 antibodies and the recombinant protein was measured  
462 by ELISA assay. Incubations of recEcRBLL-1 (25 µg mL<sup>-1</sup>) or anti-EcRBLL-1 (1:100)  
463 with MRC-5 cells showed a decrease in the growth of *E. cuniculi* with inhibition  
464 percentages ranging from 12.3% to 23.7% (Fig. 5, Supplementary data Fig. S2 and  
465 S3). Indeed, when cells were put in contact with anti-EcRBLL-1 and were infected  
466 with 2 x 10<sup>5</sup> spores, a decrease on average of 12.3% in the growth of the parasite  
467 was observed. In parallel, a pretreatment of cells with recEcRBLL-1 infected at 2 x  
468 10<sup>5</sup> spores led to a reduction on average of 23.7% of the parasite growth ( *p* < 0.001).

469 The involvement of AaRBLL-1 and AaRBLL-2 in spore adherence and infection was  
470 analyzed as described previously. The growth inhibition of *A. algerae* was quantified  
471 by using fluorescence *in situ* hybridization (FISH) method. Cell nuclei and infectious  
472 foci in 10 randomly chosen fields from each coverslip were counted in order to  
473 assess the percentage of infected cells over total cells. A pre-treatment with anti-  
474 AaRBLL-1 and anti-AaRBLL-2 polyclonal antibodies or the recombinant protein



475 recAaRBLL-2 decreased the proliferation of the parasite on average by 67.6%,  
476 68.5%, and 59.3% respectively (Fig. 6). No pre-treatment with recAaRBLL-1 was  
477 done as the insoluble recombinant protein was purified in denaturing conditions.

478

#### 479 **4. Discussion**

480 The adherence of intracellular parasites to host cell is the first step of the infection  
481 process. In Microsporidia, spore wall and polar tube proteins play an important role in  
482 the interaction between spores and host cells [27]. Several proteins that can interact  
483 with host cells have already been described in particular in *N. bombycis*,  
484 *Encephalitozoon spp.*, and *A. locustae* [23–28]. In the present study, candidate  
485 proteins from *E. cuniculi* and *A. algerae* were selected based on the prediction on  
486 several motifs such as signal peptide and a Ricin-B-lectin like domain.

487 The results of subcellular localization and glycosylation site prediction showed that  
488 EcRBLL-1 and AaRBLL-2 are potential secreted proteins and that all three proteins  
489 may bind to carbohydrates. However, only AaRBLL-1 does not possess a signal  
490 peptide that could be explained by the fact that the algorithms used (WoLF PSORT  
491 and SignalP) have been set up on genetics models which are not completely adapted  
492 to Microsporidia. In this way, the protein SWP12 from *N. bombycis* was shown to be  
493 present at the spore coat by IFA even though no signal peptide was predicted  
494 [45,46]. The three selected proteins possess a Ricin-B-lectin domain known to be  
495 important in parasite adherence and infection in Microsporidia [32,33]. The analysis  
496 of RBL proteins in microsporidian species revealed a large heterogeneity in  
497 sequences but also no significant analogy between the protein sequences found  
498 within a same species. However, the presence of common structures in the RBLL  
499 proteins, in particular like in agglutinin and  $\beta$ -glucanase, could be linked to the

500 conservation of the function of carbohydrate binding as exemplified by the 3D  
501 prediction model (Table 1). The comparison of *A. algerae* and *E. cuniculi* proteomes  
502 revealed a greater number of RBL proteins in *A. algerae* proteome (~17 for *A.*  
503 *algerae* versus 6 for *E. cuniculi*). The RBL protein encoding genes are found in other  
504 microsporidian species, *N. ceranae* and *S. lophii*, respectively parasites of  
505 honeybees and monkfish and are organized as clusters in genome sequences. It is  
506 also the case for *E. cuniculi* as RBLL genes are found in syntenic blocks including  
507 our *EcRBLL-1* gene [32]. The low size of *A. algerae* genome contigs did not allow us  
508 to analyze RBLL gene synteny in this genome. Campbell et al., 2013 [32]  
509 hypothesized that RBL paralogs have arisen from duplication in each species and  
510 may have contributed to host adaptation. Hence, this difference in the number of  
511 proteins present in *A. algerae* and *E. cuniculi* could be linked to the broad host range  
512 of *A. algerae* going from mammals to insects.

513 The results of immunolocalization on *E. cuniculi* and *A. algerae* spores and polar tube  
514 demonstrate a heterogeneity of labelling. The difference of localizations of the three  
515 proteins (dual localization on polar tube and the spore wall for *A. algerae* and  
516 restricted to polar tube for *E. cuniculi*) argues for the fact that they are probably  
517 functionally different during the invasion process. The more intensive labeling of  
518 *EcRBLL-1* at the tip ~~polar tube~~ has questioned about the role of this protein in the  
519 attachment to the host cell membrane before the piercing of the polar tube. This  
520 could correspond to the tip of the polar tube or to the sporoplasm. A specific  
521 sporoplasm marker needs to be developed to answer this question. Transmission  
522 electron microscopy will also be helpful to address this questioning. The *A. algerae*  
523 and *E. cuniculi* RBLLs may be also different from the one identified in *N. bombycis*  
524 [33] as *NbRBL* was only localized at the spore wall. Despite these differences, they

525 are all involved in the host cell infection, as a significant decrease of *E. cuniculi* and  
526 *A. algerae* proliferation was observed after pre-treatments of host cells with  
527 recombinant proteins or microsporidian spores with polyclonal anti-RBLL proteins.  
528 These results were consistent with previous results observed for *Nb*RBL binding to  
529 carbohydrates and contributing to spore adherence [33]. Indeed, RBL proteins could  
530 be released during spore germination as the spore content is passing through the  
531 polar tube. *Ec*RBLL-1, *Aa*RBLL-1 and *Aa*RBLL-2 could then contribute to the  
532 anchoring of the polar tube, by binding to host cells carbohydrates by means of the  
533 Ricin-B-Lectin domain. The distance between host cell and spores being shorter for  
534 germination, the sporoplasm would be internalized by endocytic mechanism into the  
535 host cell ([Supplementary data Figure S1](#)).

536 However, *Ec*RBLL-1, *Aa*RBLL-1 and *Aa*RBLL-2 did not abolish the infection  
537 indicating the involvement of other components in the molecular basis of spore  
538 adherence. These proteins all possess a Ricin B Lectin region and it has been shown  
539 that this lectin interacts with glycolipids or glycoproteins on cell surface [35,36]. Once  
540 the lectin has interacted with sugar moieties of host cells, it is presumably imported  
541 into endosomes into the cytosol of host cells [34].

542 RBL [proteins](#) are described as glycoproteins composed of two chains, a chain A  
543 involved in the inhibition of protein synthesis and a chain B (lectin) interacting with  
544 glycoproteins and glycolipids at the cell surface [36,47]. Ricin-B Lectins can be  
545 involved in different mechanisms such as protein activity inhibition, apoptosis  
546 pathways or release of cytokine inflammatory mediators [47]. Several pathogens  
547 synthesize lectins often reported to be interacting with glycoconjugates on host cells  
548 promoting cell adherence, invasion and colonization of host cells [48–51].  
549 *Entamoeba histolytica* trophozoites, an enteric protozoan parasite, possess a cell

550 surface lectin mediating the adherence of the parasite to host galactose and N-  
551 acetyl-D-galactosamine [52,53]. The secreted Microneme (MICs) and rhoptry  
552 proteins (ROPs and RONs) of the protozoan parasite, *Toxoplasma gondii* play an  
553 important role in host cell recognition, attachment and penetration [54]. Two MICs  
554 proteins, MIC1 and MIC4, have lectin domains capable of binding to oligosaccharides  
555 with sialic acid and D-galactose in the terminal position, respectively [48,55–58].  
556 However, the molecular mechanism of RBL interaction with host cells is unknown in  
557 Microsporidia.

558 To conclude and in order to further understand the infection process, it would be  
559 interesting to identify potential cellular receptors targeted by microsporidian RBLLs at  
560 the host cell surface using technics allowing the identification of protein-protein  
561 interactions such as co-immunoprecipitation or pull-down approaches. In parallel,  
562 functional approaches based on RNAi could help to better understand the role of the  
563 RBLL proteins in adherence and infection processes in Microsporidia. Huang in 2018  
564 [59] demonstrated that *A. algerae* is one of the microsporidian species that possess  
565 RNA interference (RNAi) genes and could therefore constitute an appropriate model  
566 for such an approach. Few studies have investigated the efficiency of using siRNA  
567 targeting specific genes in Microsporidia, mainly in *N. ceranae* and *Heterosporis*  
568 *saurida*, microsporidian parasites of honeybee and lizardfish respectively [60,61].  
569 Finally, our findings contribute to the deciphering of the adherence of *E. cuniculi* and  
570 *A. algerae* to host cells, in which *EcRBLL-1*, *AaRBLL-1* and *AaRBLL-2* may play a  
571 significant role and could pave the way to develop new therapeutic/prophylactic  
572 methods to control these intracellular parasites.

573

574 **Declaration of interest**

575 The authors declare no conflict of interest

576

### 577 **Acknowledgments**

578 This work has been supported by a grant (MENRT) of the Ministère de  
579 l'Enseignement Supérieur et de la Recherche, attributed to PhD student.

580 We thank Ivan Wawrzyniack from the LMGE of University Clermont-Auvergne  
581 (France) for his contribution to the genome data analysis of microsporidian species.

582

### 583 **References**

584

- 585 [1] A. Cali, J.J. Becnel, P.M. Takvorian, *Microsporidia*, 2nd ed., Springer  
586 International Publishing, 2017. [https://doi.org/10.1007/978-3-319-32669-6\\_27-1](https://doi.org/10.1007/978-3-319-32669-6_27-1).
- 587 [2] K.W. Nägeli, Über die neue krankheit der Seidenraupe und verwandte  
588 organismen, *Bot. Z.* 15 (1857) 760–761.
- 589 [3] J. Vávra, J. Lukeš, *Microsporidia and ‘The Art of Living Together,’* in: D.  
590 Rollinson (Ed.), *Adv. Parasitol.*, 1st editio, Elsevier Ltd, 2013: pp. 253–319.  
591 <https://doi.org/10.1016/B978-0-12-407706-5.00004-6>.
- 592 [4] A. Cali, P.M. Takvorian, *Developmental Morphology and Life Cycles of the*  
593 *Microsporidia*, in: L.M. Weiss, J.J. Becnel (Eds.), *Microsporidia Pathog. Oppor.*,  
594 1st ed., John Wiley & Sons, Inc., 2014: pp. 71–133.  
595 <https://doi.org/10.1002/9781118395264.ch2>.
- 596 [5] E.S. Didier, K.F. Snowden, J.A. Shadduck, *Biology of microsporidian species*  
597 *infecting mammals*, Academic Press Limited, 1998.  
598 [https://doi.org/10.1016/S0065-308X\(08\)60125-6](https://doi.org/10.1016/S0065-308X(08)60125-6).
- 599 [6] M. Wittner, L.M. Weiss, *The Microsporidia and Microsporidiosis*, American  
600 Society of Microbiology Press, 1999. <https://doi.org/10.1128/9781555818227>.
- 601 [7] G.D. Stentiford, J.J. Becnel, L.M. Weiss, P.J. Keeling, E.S. Didier, B.A.P.  
602 Williams, S. Bjornson, M.L. Kent, M.A. Freeman, M.J.F. Brown, E.R. Troemel,  
603 K. Roesel, Y. Sokolova, K.F. Snowden, L. Solter, *Microsporidia – Emergent*  
604 *Pathogens in the Global Food Chain*, *Trends Parasitol.* 32 (2016) 336–348.  
605 <https://doi.org/10.1016/j.pt.2015.12.004>.
- 606 [8] L.M. Weiss, T.D. Edlind, C.R. Vossbrinck, T. Hashimoto, *Microsporidian*  
607 *molecular phylogeny: the fungal connection.*, *J. Eukaryot. Microbiol.* 46 (1999)  
608 17S-18S.
- 609 [9] S.C. Lee, N. Corradi, E.J. Byrnes lii, S. Torres-Martinez, F.S. Dietrich, P.J.

- 610 Keeling, J. Heitman, Microsporidia evolved from ancestral sexual fungi, *Curr.*  
611 *Biol.* 18 (2008) 1675–1679. <https://doi.org/10.1016/j.cub.2008.09.030>.
- 612 [10] S. Capella-Gutiérrez, M. Marcet-Houben, T. Gabaldón, Phylogenomics  
613 supports microsporidia as the earliest diverging clade of sequenced fungi, *BMC*  
614 *Biol.* 10 (2012). <https://doi.org/10.1186/1741-7007-10-47>.
- 615 [11] D. Corsaro, J. Walochnik, D. Venditti, J. Steinmann, K.-D. Müller, R. Michel,  
616 Microsporidia-like parasites of amoebae belong to the early fungal lineage  
617 Rozellomycota, *Parasitol. Res.* 113 (2014) 1909–1918.  
618 <https://doi.org/10.1007/s00436-014-3838-4>.
- 619 [12] P.J. Keeling, Phylogenetic Place of Microsporidia in the Tree of Eukaryotes, in:  
620 L.M. Weiss, J.J. Becnel (Eds.), *Microsporidia Pathog. Oppor.*, 1st editio, John  
621 Wiley & Sons, Inc., 2014: pp. 195–202.  
622 <https://doi.org/10.1002/9781118395264.ch5>.
- 623 [13] J.P. Kramer, Longevity of microsporidian spores with special reference to  
624 *Octosporea muscaedomesticae* flu, *Acta Protozool.* 8 (1970) 217–224.
- 625 [14] J. Vávra, J.I.R. Larsson, Chapter 1: Structure of Microsporidia, in: L.M. Weiss,  
626 J.J. Becnel (Eds.), *Microsporidia Pathog. Oppor.*, First edit, John Wiley & Sons,  
627 Inc., 2014: pp. 1–70. <https://doi.org/10.1002/9781118395264.ch1>.
- 628 [15] G.J. Leitch, G.S. Visvesvara, Q. He, Inhibition of microsporidian spore  
629 germination, *Parasitol. Today.* 9 (1993) 422–424. [https://doi.org/10.1016/0169-](https://doi.org/10.1016/0169-4758(93)90052-H)  
630 [4758\(93\)90052-H](https://doi.org/10.1016/0169-4758(93)90052-H).
- 631 [16] J. Schottelius, C. Schmetz, N.P. Kock, T. Schüler, I. Sobottka, B. Fleischer,  
632 Presentation by scanning electron microscopy of the life cycle of microsporidia  
633 of the genus *Encephalitozoon*, *Microbes Infect.* 2 (2000) 1401–1406.  
634 [https://doi.org/10.1016/S1286-4579\(00\)01293-4](https://doi.org/10.1016/S1286-4579(00)01293-4).

- 635 [17] G.J. Leitch, C. Ceballos, Effects of host temperature, and gastric and duodenal  
636 environments on microsporidia spore germination and infectivity of intestinal  
637 epithelial cells, *Parasitol. Res. Res.* 104 (2008) 35–42.  
638 <https://doi.org/10.1007/s00436-008-1156-4>.
- 639 [18] Y. Xu, L.M. Weiss, The microsporidian polar tube: A highly specialised invasion  
640 organelle, *Int. J. Parasitol.* 35 (2005) 941–953.  
641 <https://doi.org/10.1016/j.ijpara.2005.04.003>.
- 642 [19] A.H. Undeen, S.W. Avery, Germination of experimentally nontransmissible  
643 microsporidia, *J. Invertebr. Pathol.* 43 (1984) 299–301.  
644 [https://doi.org/10.1016/0022-2011\(84\)90156-3](https://doi.org/10.1016/0022-2011(84)90156-3).
- 645 [20] A.H. Undeen, N.D. Epsky, In vitro and in vivo germination of *Nosema locustae*  
646 (*Microspora: Nosematidae*) spores, *J. Invertebr. Pathol.* 56 (1990) 371–379.  
647 [https://doi.org/10.1016/0022-2011\(90\)90124-O](https://doi.org/10.1016/0022-2011(90)90124-O).
- 648 [21] E. Frixione, L. Ruiz, A.H. Undeen, Monovalent cations induce microsporidian  
649 spore germination in vitro, *J. Euk. Microbiol.* 41 (1994) 464–468.  
650 <https://doi.org/10.1111/j.1550-7408.1994.tb06043.x>.
- 651 [22] F. Delbac, V. Polonais, The microsporidian polar tube and its role in invasion,  
652 *Subcell. Biochem.* 47 (2008) 208–220. [https://doi.org/10.1007/978-0-387-](https://doi.org/10.1007/978-0-387-78267-6_17)  
653 [78267-6\\_17](https://doi.org/10.1007/978-0-387-78267-6_17).
- 654 [23] L. Chen, R. Li, Y. You, K. Zhang, L. Zhang, A Novel Spore Wall Protein from  
655 *Antonospora locustae* (*Microsporidia: Nosematidae*) Contributes to Sporulation,  
656 *J. Eukaryot. Microbiol.* 64 (2017) 779–791. <https://doi.org/10.1111/jeu.12410>.
- 657 [24] J.R. Hayman, S.F. Hayes, J. Amon, T.E. Nash, Developmental expression of  
658 two spore wall proteins during maturation of the microsporidian  
659 *Encephalitozoon intestinalis*, *Infect. Immun.* 69 (2001) 7057–7066.



- 660 <https://doi.org/10.1128/IAI.69.11.7057-7066.2001>.
- 661 [25] J.R. Hayman, T.R. Southern, T.E. Nash, Role of sulfated glycans in adherence  
662 of the microsporidian *Encephalitozoon intestinalis* to host cells in vitro, *Infect.*  
663 *Immun.* 73 (2005) 841–848. <https://doi.org/10.1128/IAI.73.2.841-848.2005>.
- 664 [26] Y. Li, Z. Wu, G. Pan, W. He, R. Zhang, J. Hu, Z. Zhou, Identification of a novel  
665 spore wall protein (SWP26) from microsporidia *Nosema bombycis*, *Int. J.*  
666 *Parasitol.* 39 (2009) 391–398. <https://doi.org/10.1016/j.ijpara.2008.08.011>.
- 667 [27] T.R. Southern, C.E. Jolly, M.E. Lester, J.R. Hayman, EnP1, a microsporidian  
668 spore wall protein that enables spores to adhere to and infect host cells in vitro,  
669 *Euk. Cell.* 6 (2007) 1354–1362. <https://doi.org/10.1128/EC.00113-07>.
- 670 [28] Z. Wu, Y. Li, G. Pan, Z. Zhou, Z. Xiang, SWP25, a novel protein associated  
671 with the *Nosema bombycis* endospore, *J. Euk. Microbiol.* 56 (2009) 113–118.  
672 <https://doi.org/10.1111/j.1550-7408.2008.00375.x>.
- 673 [29] C.A. Leonard, *Microsporidia Spore Adherence and Host Cell Infection In Vitro*,  
674 East Tennessee State University, 2013.
- 675 [30] F. Zhu, Z. Shen, J. Hou, J. Zhang, T. Geng, X. Tang, L. Xu, X. Guo,  
676 Identification of a protein interacting with the spore wall protein SWP26 of  
677 *Nosema bombycis* in a cultured BmN cell line of silkworm, *Infect. Genet. Evol.*  
678 17 (2013) 38–45. <https://doi.org/10.1016/j.meegid.2013.03.029>.
- 679 [31] B. Han, V. Polonais, T. Sugi, R. Yakubu, P.M. Takvorian, A. Cali, K. Maier, M.  
680 Long, M. Levy, H.B. Tanowitz, G. Pan, F. Delbac, Z. Zhou, L.M. Weiss, The  
681 role of microsporidian polar tube protein 4 (PTP4) in host cell infection, *PLoS*  
682 *Pathog.* 13 (2017) 1–28. <https://doi.org/10.1371/journal.ppat.1006341>.
- 683 [32] S.E. Campbell, T.A. Williams, A. Yousuf, D.M. Soanes, K.H. Paszkiewicz,  
684 B.A.P. Williams, The Genome of *Spraguea lophii* and the Basis of Host-

- 685 Microsporidian Interactions, *PLoS Genet.* 9 (2013) 1–15.  
686 <https://doi.org/10.1371/journal.pgen.1003676>.
- 687 [33] H. Liu, M. Li, S. Cai, X. He, Y. Shao, X. Lu, Ricin-B-lectin enhances  
688 microsporidia *Nosema bombycis* infection in BmN cells from silkworm *Bombyx*  
689 *mori*, *Acta Biochim. Biophys. Sin.* 48 (2016) 1050–1057.  
690 <https://doi.org/10.1093/abbs/gmw093>.
- 691 [34] R.D. Cummings, R.L. Schnaar, R-Type Lectins, in: A. Varki, R. Cummings, J.  
692 Esko, H. Freeze, G. Hart, J. Marth (Eds.), *Essentials Glycobiol.*, 3rd ed., Cold  
693 Spring Harbor Laboratory Press, Cold Spring Harbor (NY), 2017.  
694 <https://doi.org/10.1101/glycobiology.3e.031>.
- 695 [35] K. Sandvig, Entry of ricin and Shiga toxin into cells: molecular mechanisms and  
696 medical perspectives, *EMBO J.* 19 (2000) 5943–5950.  
697 <https://doi.org/10.1093/emboj/19.22.5943>.
- 698 [36] S. Olsnes, The history of ricin, abrin and related toxins, *Toxicon.* 44 (2004)  
699 361–370. <https://doi.org/10.1016/j.toxicon.2004.05.003>.
- 700 [37] A. Varki, R. Cummings, J. Esko, H. Freeze, G. Hart, J. Marth, Part IV, Glucan-  
701 binding Proteins, in: A. Varki, R. Cummings, J. Esko, H. Freeze, G. Hart, J.  
702 Marth (Eds.), *Essentials Glycobiol.*, 2nd ed., Cold Spring Harbor Laboratory  
703 Press, 2009. <https://www.ncbi.nlm.nih.gov/books/NBK20728/>.
- 704 [38] R.V. Romero, R. Osicka, P. Sebo, Filamentous hemagglutinin of *Bordetella*  
705 *pertussis*: A key adhesin with immunomodulatory properties?, *Futur. Microbiol.*  
706 9 (2014) 1339–1360. <https://doi.org/10.2217/fmb.14.77>.
- 707 [39] S.M. Prasad, Y. Yin, E. Rodzinski, E.I. Tuomanen, H. Robert Masure,  
708 Identification of a Carbohydrate Recognition Domain in Filamentous  
709 Hemagglutinin from *Bordetella pertussis*, *Infect. Immun.* 61 (1993) 2780–2785.

- 710 <https://doi.org/10.1128/iai.61.7.2780-2785.1993>.
- 711 [40] E. Tuomanen, H. Towbin, G. Rosenfelder, D. Braun, G. Larson, S. Gunnar, C.  
712 Hansson, R. Hilli, Receptor analogs and monoclonal antibodies that inhibit  
713 adherence of *Bordetella Pertussis* to human ciliated respiratory epithelial cells,  
714 *J. Exp. Med.* 168 (1988) 267–277. <https://doi.org/10.184/jem.168.1.267>.
- 715 [41] W.H. Tham, J. Healer, A.F. Cowman, Erythrocyte and reticulocyte binding-like  
716 proteins of *Plasmodium falciparum*, *Trends Parasitol.* 28 (2012) 23–30.  
717 <https://doi.org/10.1016/j.pt.2011.10.002>.
- 718 [42] J.D. Esko, N. Sharon, *Microbial Lectins: Hemagglutinins, Adhesins, and*  
719 *Toxins.*, in: A. Varki, R.D. Cummings, J.D. Esko, H.H. Freeze, P. Stanley, C.R.  
720 Bertozzi, G.W. Hart, M.E. Etzler (Eds.), *Essentials Glycobiol.*, 2nd Ed., Cold  
721 Spring Harbor Laboratory Press, Cold Spring Harbor (NY), 2009.
- 722 [43] A.J. Thompson, L. Cao, Y. Ma, X. Wang, J.K. Diedrich, C. Kikuchi, S. Willis, C.  
723 Worth, R. McBride, J.R. Yates, J.C. Paulson, Human Influenza Virus  
724 Hemagglutinins Contain Conserved Oligomannose N-Linked Glycans Allowing  
725 Potent Neutralization by Lectins, *Cell Host Microbe.* 27 (2020) 1–11.  
726 <https://doi.org/10.1016/j.chom.2020.03.009>.
- 727 [44] G.N. Rogers, J.C. Paulson, Receptor Determinants of Human and Animal  
728 Influenza Virus Isolates: Differences in Receptor Specificity of the H3  
729 Hemagglutinin Based on Species of Origin, *Virology.* 127 (1983) 361–373.  
730 [https://doi.org/10.1016/0042-6822\(83\)90150-2](https://doi.org/10.1016/0042-6822(83)90150-2).
- 731 [45] J. Chen, L. Geng, M. Long, T. Li, Z. Li, D. Yang, C. Ma, H. Wu, Z. Ma, C. Li, G.  
732 Pan, Z. Zhou, Identification of a novel chitin-binding spore wall protein  
733 (NbSWP12) with a BAR-2 domain from *Nosema bombycis* (microsporidia),  
734 *Parasitology.* 140 (2013) 1394–1402.

735 <https://doi.org/10.1017/S0031182013000875>.

736 [46] Z. Wu, Y. Li, G. Pan, X. Tan, J. Hu, Z. Zhou, Z. Xiang, Proteomic analysis of  
737 spore wall proteins and identification of two spore wall proteins from *Nosema*  
738 *bombycis* (Microsporidia), *Proteomics*. 8 (2008) 2447–2461.  
739 <https://doi.org/10.1002/pmic.200700584>.

740 [47] J. Audi, M. Belson, M. Patel, J. Schier, J. Osterloh, Ricin Poisoning, *Jama*. 294  
741 (2005) 2342–2351. <https://doi.org/10.1001/jama.294.18.2342>.

742 [48] A. Sardinha-Silva, F. Mendonça-Natividade, C. Pinzan, C. Lopes, D. Costa, D.  
743 Jacot, F. Fernandes, A. Zorzetto-Fernandes, N. Gay, A. Sher, D. Jankovic, D.  
744 Soldati-Favre, M. Grigg, M.C. Roque-Barreira, The lectin-specific activity of  
745 *Toxoplasma gondii* microneme proteins 1 and 4 binds Toll-like receptor 2 and 4  
746 N-glycans to regulate innate immune priming, *PLoS Pathog*. 15 (2019) 1–24.  
747 <https://doi.org/10.1371/journal.ppat.1007871>.

748 [49] P.M. Nogueira, R.R. Assis, A.C. Torrecilhas, E.M. Saraiva, N.L. Pessoa, M.A.  
749 Campos, E.F. Marialva, C.M. Ríos-Velasquez, F.A. Pessoa, N.F. Secundino,  
750 J.N. Rugani, E. Nieves, S.J. Turco, M.N. Melo, R.P. Soares,  
751 Lipophosphoglycans from *Leishmania amazonensis* Strains Display  
752 Immunomodulatory Properties via TLR4 and Do Not Affect Sand Fly Infection,  
753 *PLoS Negl. Trop. Dis.* 10 (2016) 1–17.  
754 <https://doi.org/10.1371/journal.pntd.0004848>.

755 [50] M.A. Favila, N.S. Geraci, A. Jayakumar, S. Hickerson, J. Mostrom, S.J. Turco,  
756 S.M. Beverley, M.A. McDowell, Differential impact of LPG-and PG-deficient  
757 *Leishmania major* mutants on the immune response of human dendritic cells,  
758 *PLoS Negl. Trop. Dis.* 9 (2015) 1–28.  
759 <https://doi.org/10.1371/journal.pntd.0004238>.

- 760 [51] K.E.M. Persson, F.J. McCallum, L. Reiling, N.A. Lister, J. Stubbs, A.F.  
761 Cowman, K. Marsh, J.G. Beeson, Variation in use of erythrocyte invasion  
762 pathways by *Plasmodium falciparum* mediates evasion of human inhibitory  
763 antibodies, *J. Clin. Invest.* 118 (2008) 342–351.  
764 <https://doi.org/10.1172/JCI32138>.
- 765 [52] W.A. Petri, R. Haque, B.J. Mann, The bittersweet interface of parasite and  
766 host: Lectin-carbohydrate interactions during human invasion by the parasite  
767 *Entamoeba histolytica*, *Ann.Rev. Microbio.* 56 (2002) 39–64.  
768 <https://doi.org/10.1146/annurev.micro.56.012302.160959>.
- 769 [53] W.A. Petri, R.D. Smith, P.H. Schlesinger, C.F. Murphy, J.I. Ravdin, Isolation of  
770 the galactose-binding lectin that mediates the in vitro adherence of *Entamoeba*  
771 *histolytica*, *J. Clin. Invest.* 80 (1987) 1238–1244.  
772 <https://doi.org/10.1172/JCI113198>.
- 773 [54] V.B. Carruthers, L.D. Sibley, Sequential protein secretion from three distinct  
774 organelles of *Toxoplasma gondii* accompanies invasion of human fibroblasts,  
775 *Eur. J. Cell Biol.* 73 (1997) 114–23.
- 776 [55] T.M.A. Blumenschein, N. Friedrich, R.A. Childs, S. Saouros, E.P. Carpenter,  
777 M.A. Campanero-Rhodes, P. Simpson, W. Chai, T. Koutroukides, M.J.  
778 Blackman, T. Feizi, D. Soldati-Favre, S. Matthews, Atomic resolution insight  
779 into host cell recognition by *Toxoplasma gondii*, *EMBO J.* 26 (2007) 2808–  
780 2820. <https://doi.org/10.1038/sj.emboj.7601704>.
- 781 [56] S. Brecht, V.B. Carruthers, D.J.P. Ferguson, O.K. Giddings, G. Wang, U. Jäkle,  
782 J.M. Harper, L.D. Sibley, D. Soldati, The *Toxoplasma* Micronemal Protein MIC4  
783 Is an Adhesin Composed of Six Conserved Apple Domains, *J. Biol. Chem.* 276  
784 (2001) 4119–4127. <https://doi.org/10.1074/jbc.M008294200>.

- 785 [57] E. V. Lourenço, S.R. Pereira, V.M. Faça, A.A.M. Coelho-Castelo, J.R. Mineo,  
786 M.C. Roque-Barreira, L.J. Greene, A. Panunto-Castelo, *Toxoplasma gondii*  
787 micronemal protein MIC1 is a lactose-binding lectin, *Glycobiology*. 11 (2001)  
788 541–547. <https://doi.org/10.1093/glycob/11.7.541>.
- 789 [58] J. Marchant, B. Cowper, Y. Liu, L. Lai, C. Pinzan, J.B. Marq, N. Friedrich, K.  
790 Sawmynaden, L. Liew, W. Chai, R.A. Childs, S. Saouros, P. Simpson, M.C.R.  
791 Barreira, T. Feizi, D. Soldati-Favre, S. Matthews, Galactose recognition by the  
792 apicomplexan parasite *Toxoplasma gondii*, *J. Biol. Chem.* 287 (2012) 16720–  
793 16733. <https://doi.org/10.1074/jbc.M111.325928>.
- 794 [59] Q. Huang, Evolution of Dicer and Argonaute orthologs in microsporidian  
795 parasites, *Infect. Genet. Evol.* 65 (2018) 329–332.  
796 <https://doi.org/10.1016/j.meegid.2018.08.011>.
- 797 [60] I.H. Kim, D.J. Kim, W.S. Gwak, S.D. Woo, Increased survival of the honey bee  
798 *Apis mellifera* infected with the microsporidian *Nosema ceranae* by effective  
799 gene silencing, *Arch. Insect Biochem. Physiol.* 105 (2020) 1–12.  
800 <https://doi.org/10.1002/arch.21734>.
- 801 [61] M. Saleh, G. Kumar, A.A. Abdel-Baki, M.A. Dkhil, M. El-Matbouli, S. Al-  
802 Quraishy, In Vitro Gene Silencing of the Fish Microsporidian *Heterosporis*  
803 *saurida* by RNA Interference, *Nucleic Acid Ther.* 26 (2016) 250–256.  
804 <https://doi.org/10.1089/nat.2016.0613>.
- 805

806 **Figure 1 : A) Protein sequences of *EcRBLL-1*, *AaRBLL-1*, *AaRBLL-2*.** The  
807 putative carbohydrate binding Ricin B Lectin superfamily (IPR035992) are indicated  
808 in blue. Peptide signals obtained with SignalP for *EcRBLL-1* and *AaRBLL-2* are  
809 underlined; *O*-glycosylation potential sites are indicated in bold and *N*-glycosylation in  
810 bold underlined. **B) Western Blot analysis. B) Anti- *EcRBLL-1* antibody.** In lane 1,  
811 total *E. cuniculi* spore protein extract. A signal was obtained at 28 kDa. **C) Anti-**  
812 ***AaRBLL-1* antibody and D) Anti- *AaRBLL-2* antibody.** In lane 1, total *A. algerae*  
813 spore protein extract; lane 2. **C)** A signal was obtained around 25 kDa **D)** A single  
814 signal was obtained around 20 kDa.

815

816 **Figure 2 : A) Localization of *EcRBLL-1* in *Encephalitozoon cuniculi*.** Spores  
817 were visualized using a fluorescence microscope after a first incubation with mouse  
818 polyclonal antibodies against *EcRBLL-1* followed by a second immunolabelling using  
819 an anti-*E. cuniculi* rabbit serum (from naturally infected rabbit). Fluorescence labeling  
820 demonstrated that the anti- *EcRBLL-1* polyclonal antibodies reacted with the polar  
821 tube of the spore with an unequal labelling intensity along the polar tube. The anti-*E.*  
822 *cuniculi* rabbit serum reacted as expected with the spore wall as well as the polar  
823 tube of mature spore. However, when both labeling were merged, the tip of the polar  
824 tube only reacted with the anti- *EcRBLL-1* polyclonal antibody (white arrow). **B)**  
825 **Intensity of pixels of the immuno-localization of *EcRBLL-1* in *E. cuniculi*.**  
826 Spores were visualized using a confocal microscope after incubation with antibodies  
827 against *EcRBLL-1*. Afterwards, a graph of the intensity of pixels from the image was  
828 obtained using Fiji ImageJ software to highlight the unequal localization of *EcRBLL-1*  
829 throughout the polar tube, in particular at the tip of the polar tube (white arrow). The  
830 arrowhead shows the labelling of the genetic material of the spore (in the same plane

831 as the PT labeling) using DAPI, indicating that the sporoplasm was not yet  
832 transferred through the polar tube.

833 **Figure 3 : Localization of AaRBLL-1 in *A. algerae*.** Spores were visualized using a  
834 fluorescence microscope after a first incubation with antibodies against AaRBLL-1  
835 diluted at 1:100. **A)** Brightfield allows the observation of spores and some of the polar  
836 tubes (arrows). **B)** Green fluorescence signals were observed on the spore wall  
837 (arrowheads) as well as on the polar tube (arrows).

838

839 **Figure 4 : Localization of AaRBLL-2 in *A. algerae*.** Purified spores were visualized  
840 using a fluorescence microscope after a first incubation with primary antibodies  
841 against AaRBLL-2 diluted at 1:100. **A)** Brightfield allows the observation of spores  
842 and some of the polar tubes (arrows). **B)** Green fluorescence signals were observed  
843 on polar tubes **C)** as well as on spore wall (arrowheads).

844

845 **Figure 5 : Antimicrosporidian activities of anti- *EcRBLL-1* antibody and**  
846 **rec*EcRBLL-1*.** Inhibition assay was performed using non-cytotoxic concentrations of  
847 the **A)** anti- *EcRBLL-1* antibody at 1:100 and **B)** rec*EcRBLL-1* (25  $\mu\text{g mL}^{-1}$ ) on *E.*  
848 *cuniculi*-infected MRC-5 cells. Parasite proliferation was measured 7 days post-  
849 infection. **A)** and **B)** each represent only one independent experiment from two **A)**  
850 and five **B)** replicates. Each condition was done in triplicate. Parasite proliferation  
851 was analyzed by comparing treated conditions to the infected untreated control using  
852 a Wilcox test. Differences were considered significant if the *p* value was < 0.001 (\*).  
853 **A)** A decrease on average of 12.3% in the growth of the parasite was observed when  
854 cells were infected with  $2 \times 10^5$  spores pre-treated with anti-*EcRBLL-1*. **B)** A pre-  
855 treatment of MRC-5 cells was done with 25  $\mu\text{g mL}^{-1}$  of rec*EcRBLL-1* followed by an



856 infection with  $2 \times 10^5$  spores. A reduction on average of 23.7% of parasite growth  
857 was observed.

858

859 **Figure 6 : Antimicrosporidian activities of recAaRBLL-2 and anti-AaRBLL-2,**  
860 **anti-AaRBLL-1 polyclonal antibodies.** Inhibition assay was done by pre-treating a  
861 solution of *A. algerae* spores with each polyclonal antibody at 1:100. After a quick  
862 PBS wash, spores were put in contact with HFF cells for 5 days. Parasite proliferation  
863 was then visualized by a FISH method. Results originate from 3 independent  
864 infection repeated twice. The percentage of infected cells was assessed by counting  
865 cell nuclei and infectious foci in 10 randomly chosen fields on three coverslips.  
866 Parasite proliferation was analyzed by comparing treated conditions to the infected  
867 untreated control using a Wilcox test. Differences were considered significant if the *p*  
868 value was  $< 0.001$  (\*\*). The control group are non-treated infected cells. Compared to  
869 the control group, pre-treatments with *recAaRBLL-2*, anti-AaRBLL-2 and anti-  
870 AaRBLL-1 decreased the parasite proliferation on average by 59.3%, 68.5% and  
871 67.6% respectively.

872

873

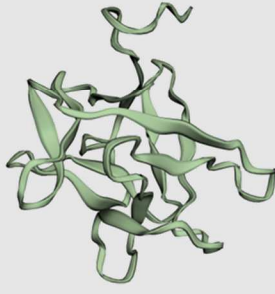
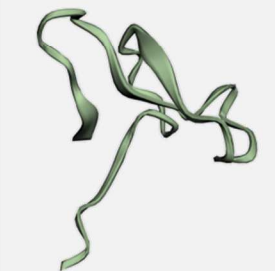
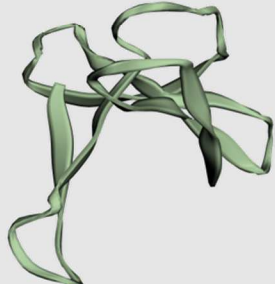
874

875

876

877

**Table 1 : Structure and functional analysis of the RBLL proteins obtained with Phyre2 online software.**

Proteins	3D model	Secondary structure	Superfamily / family /PDB molecule	Confidence	% identity
<i>EcRBLL-1</i> (ECU08_1730)		$\alpha$ helix (8%) $\beta$ strand (41%)	$\beta$ -glucanase	98.8	20
			Ricin-B-like lectin	98.6	17
			Sugar binding protein	98.4	16
			Hemagglutinin component	98.2	13
<i>AaRBLL-1</i> (MZ547653)		$\alpha$ helix (18%) $\beta$ strand (47%)	Ricin-B-like lectin	96.1	32
			Agglutinin-1 b chain	95.5	20
			Hemagglutinin component	95.3	23
			$\beta$ -glucanase	93.5	38
<i>AaRBLL-2</i> (MZ547654)		$\alpha$ helix (2%) $\beta$ strand (50%)	$\beta$ -glucanase	91.5	21
			Ricin-B-like lectin	91.4	24
			Hemagglutinin component	85.2	23
			Agglutinin	81.4	20

According to this algorithm, the likely accuracy of the model is determined by the percentage identity between our sequences and templates. Moreover, a low sequence identity (<15%) model can be useful as long as the confidence is high. A match with a confidence >90%, indicates that the protein adopts the overall fold shown in the 3D model.

A

***Ec*RBLL-1 (ECU08\_1730)**

MMLIALCMMGVVLGFKITAKNNEGKFLINNNGKAVMSESGKPAEFKTDEVSPGVKIVTDK  
NTNKVLDIEGSKTNLIFYSRHGQENQRFTFVGGEGDVIYIKSGDGCLEYSNGKMYRTTC  
SAKDQQRFKIVYSLGDPGYKPPVEVPVPAAPEN**NPST**QDLLE**SPSS**QALSGSANAHAPPQV  
LIFNGKKSHR**SHS**WHHNPYEDESSIYGSDCLIV

***Aa*RBLL-1 (MZ547653)**

MLIFFLSIKTLLIKVQNNLGFVAFDGTLYLFQTPNIKE**ASEFEFIQN**ENGIDFYIQLAKTN  
LVWDYPRQDFGGNIILYRFHGGSNQKWRLIFNKLGSLNIVNNDRRVVYNEYTNLFTTKKI  
NEYMNGEEGFVIFDEKMHYFDFFNHVPVQNIIMNVPSIEHLLPLGKELRKPS**PNIGGPSSA**  
PPIMPLGPNMHEQMFLNQMG

***Aa*RBLL-2 (MZ547654)**

MTLTKYIIILSLFINYSISFVIQERSTGRYLSSKNMGVVALVEDIRQASPYIIRAVGNP  
IDMAITDKKSKLALDFAADGPD LISYSYSSSTNQLFKLNLDENGYWQIIQGTEKYLYYDP  
ETSKLKGOPYDVSKTVGFMLFADDGIGPFVPMKGAKLP**SPI**PPVYPEAPLLPENEASFAP  
K\*

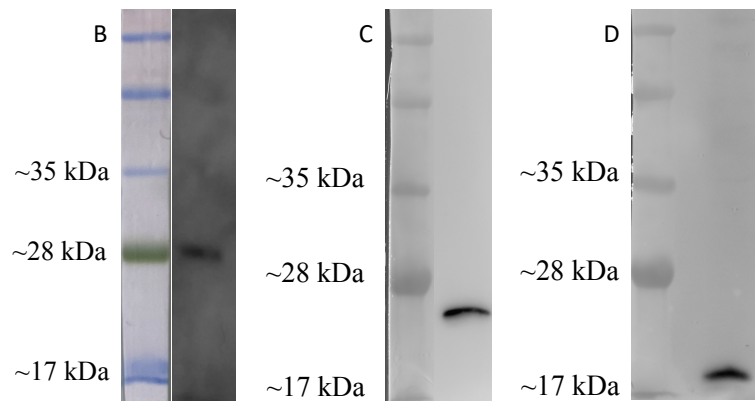


**Fig. 1**

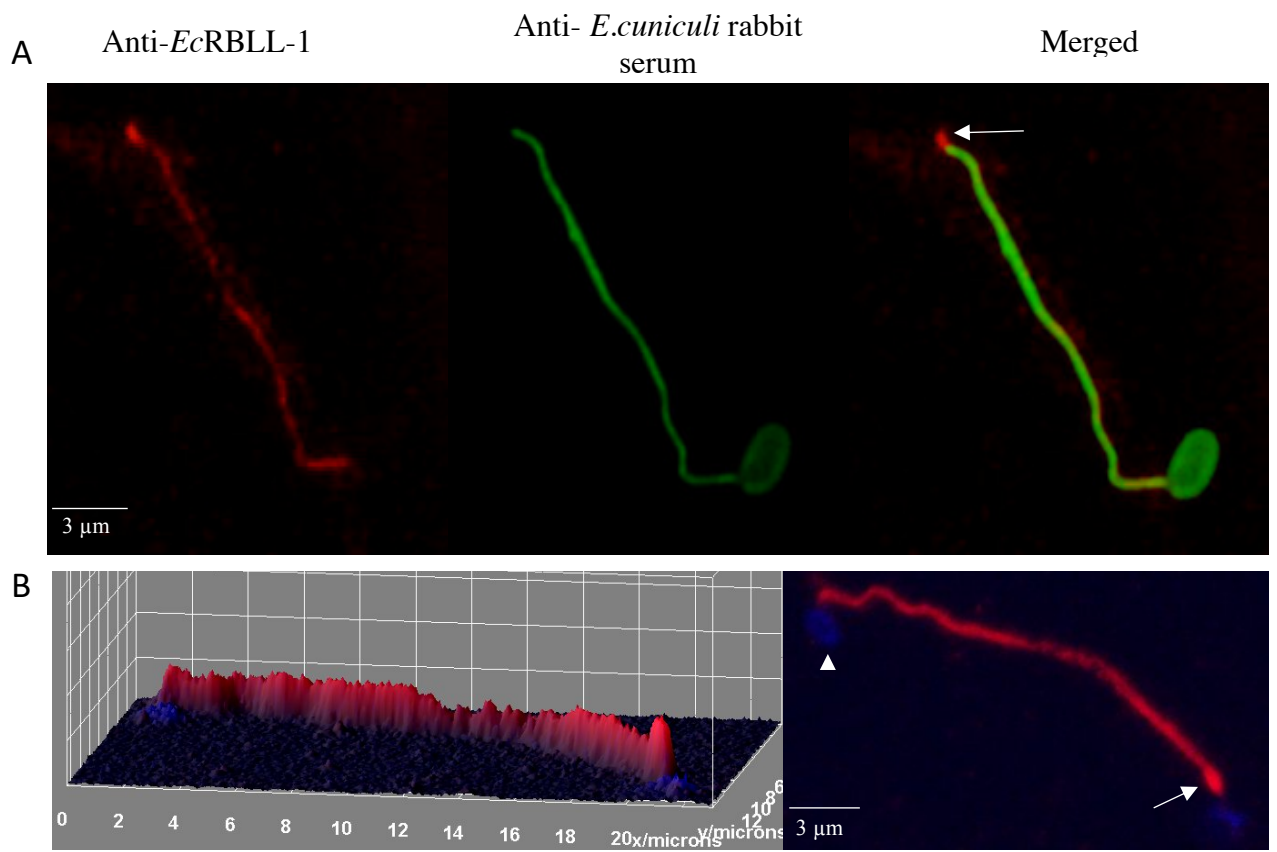


**Fig. 2**

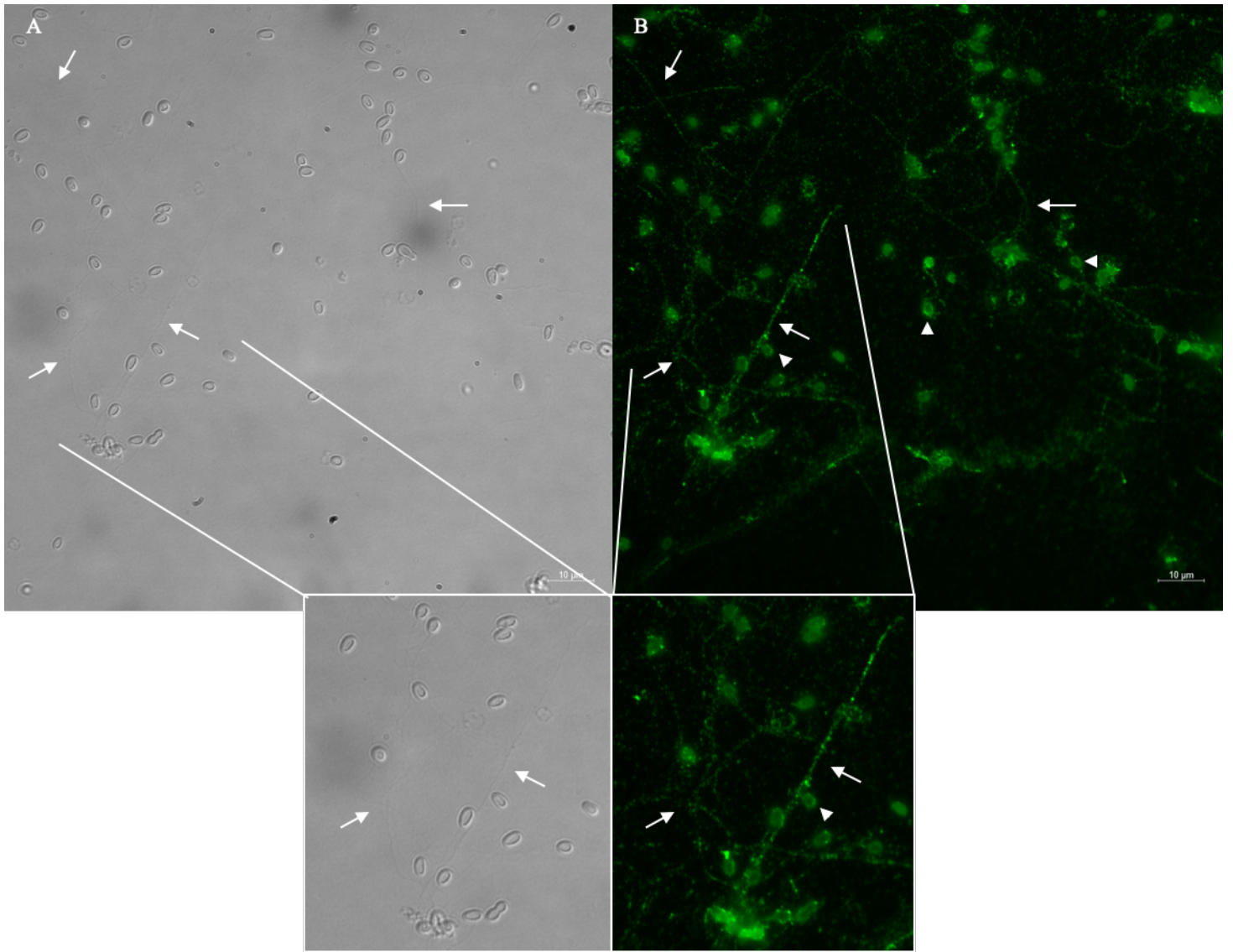


**Fig. 3**

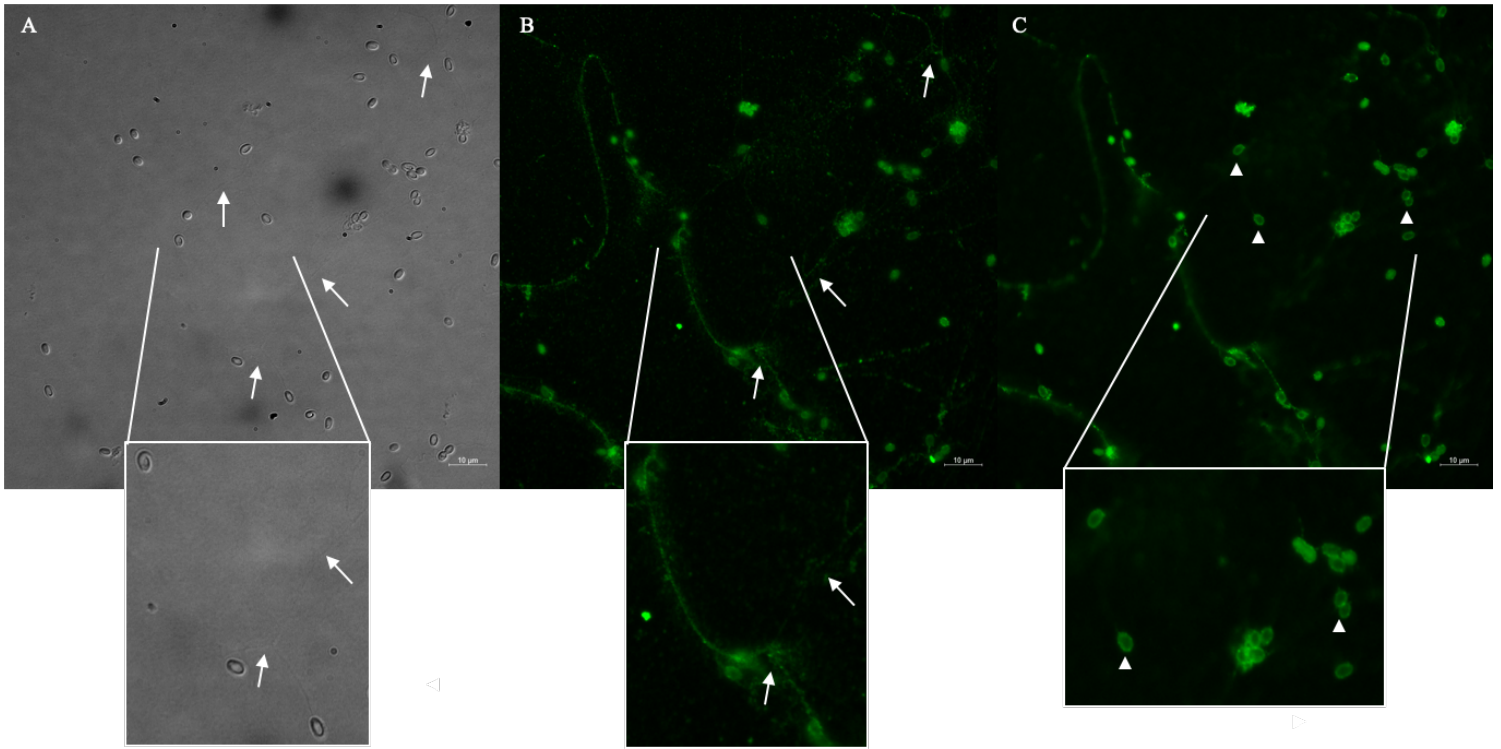


**Fig. 4**

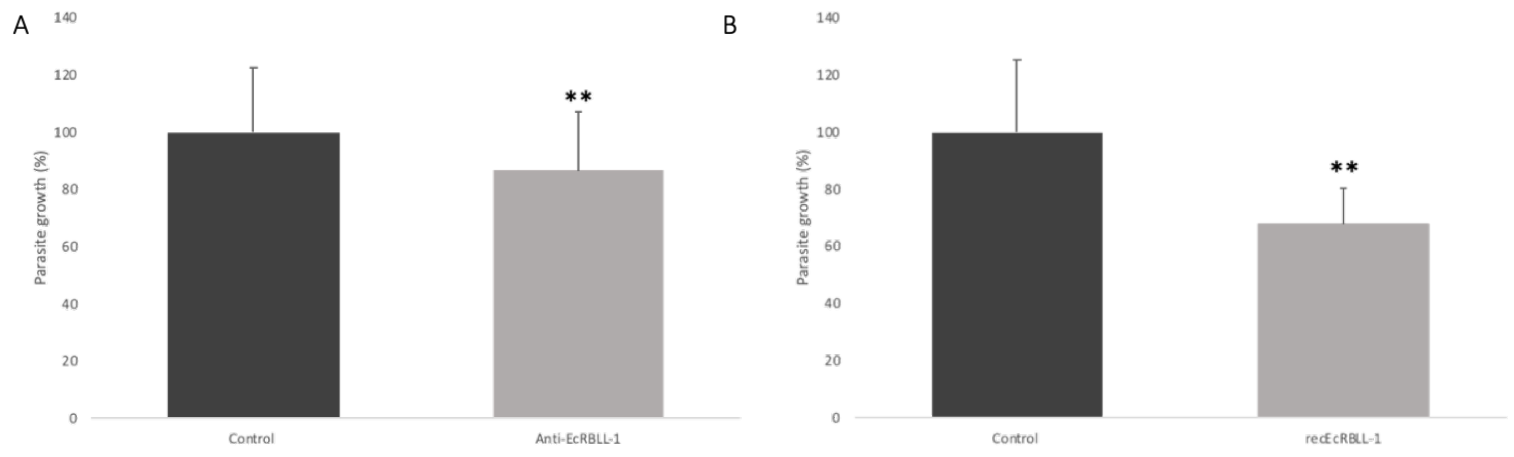


**Fig. 5**

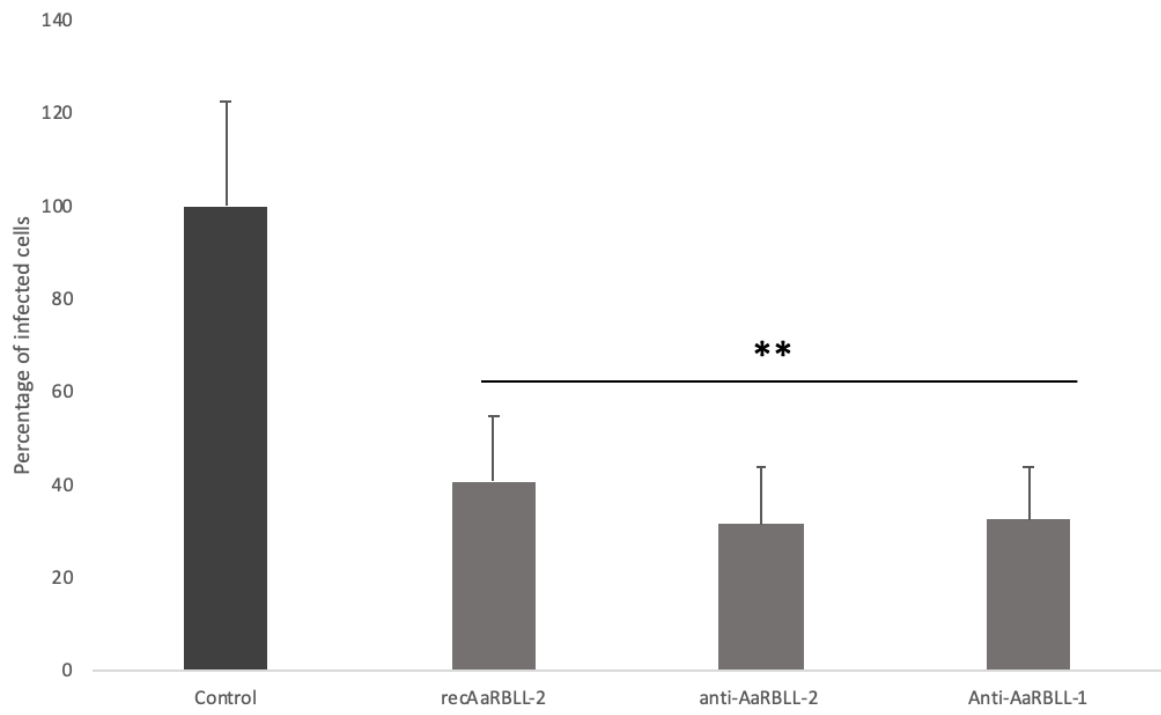
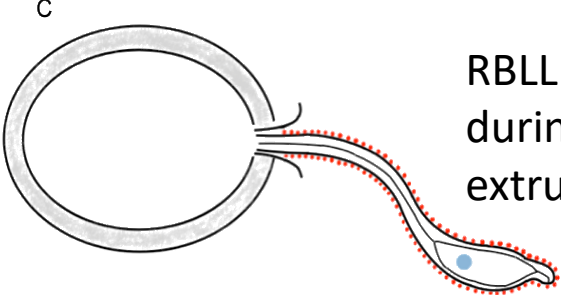
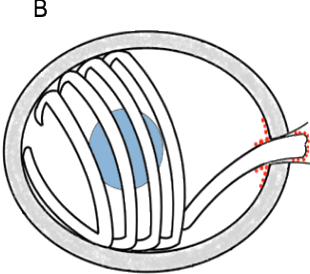
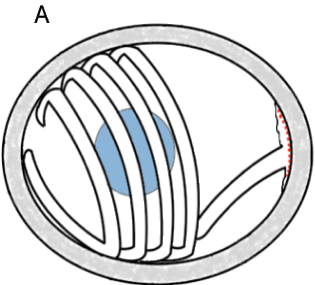


**Fig.6**



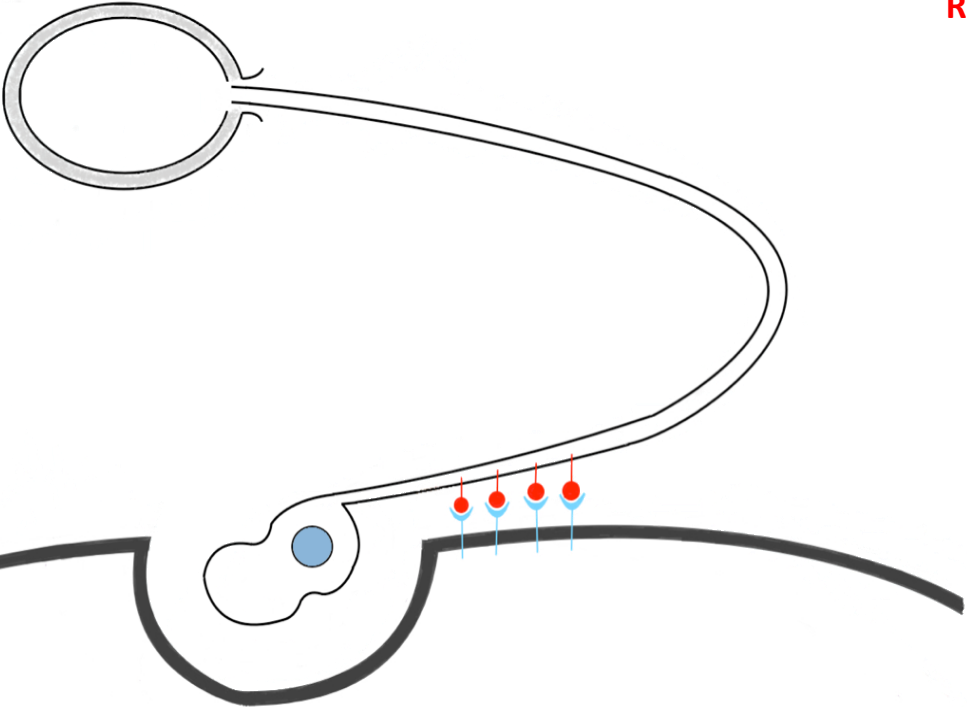
Microsporidian spore



RBLL release  
during polar tube  
extrusion

**RBLL Proteins**

D



**RBLL Proteins**

**Host cell receptors**